MICROCOPY CHART

AD-A167 842

FOREIGN TECHNOLOGY DIVISION

STUDY ON ALGORITHMS FOR PREDICTION OF SOLID PROPELLANT ROCKET MOTOR
PERFORMANCE

by

Wang Xin and Zhang Zhongqin

DTIC
ELECTE
MAY 1 9 1986
S
D
E

86 5 16 095

HUMAN TRANSLATION

FTD-ID(RS)T-0152-86   22 April 1986

MICROFICHE NR: FTD-86-C-001752

STUDY ON ALGORITHMS FOR PREDICTION OF SOLID PROPELLANT
ROCKET MOTOR PERFORMANCE

By: Wang Xin and Zhang Zhongqin

English pages: 12

Source: Hang Kong Xuebao, Vol 5, Nr. 3, September 1984,
        pp. 288-295

Country of origin: China
Translated by: FLS, INC.
               F33657-85-D-2079
Requester: FTD/SDBP
Approved for public release; Distribution unlimited.

GRAPHICS DISCLAIMER

All figures, graphics, tables, equations, etc. merged into this
translation were extracted from the best quality copy available.

Accession For

NTIS GRA&I	☒
DTIC TAB	☐
Unannounced	☐
Justification	

By

Distribution/

Availability Codes

Dist	Avail and/or Special
A-1	

QUALITY
INSPECTED
3

i

STUDY ON ALGORITHMS FOR PREDICTION OF SOLID PROPELLANT ROCKET MOTOR PERFORMANCE

Wang Xin and Zhang Zhongqin

Beijing Institute of Aeronautics and Astronautics

This article introduces two predictive algorithms for the performance of solid propellant rocket motor. The emphasis is on the introduction of Time-Space Algorithm. The authors proposed a general two-dimensional grain calculation procedure in order to conduct the grain calculations. Therefore, the predictive algorithms for performance introduced by this article show generality. A comprehensive computer program for the aforementioned method has been written and applied to calculating the performance of three different solid rocket motors. The calculated results are consistent with those derived from experimental data.

Nomenclature

a speed of sound
a_i combustion speed coefficient
a_c critical speed of sound
A_b combustion area
A_{bc} combustion area at the head
A_p passage area
A_t nozzle throat area
C_D exhaust gas coefficient
h space increment
H enthalpy
H_p enthalpy of propellant
$\dot{m}$ mass flow rate
n pressure index
p combustion gas pressure

r combustion speed of propellant
R gas constant
T combustion gas temperature
Q circumference of combustion
T_a adiabatic combustion temperature
t time
u combustion gas speed
x axial coordinate
γ specific heat ratio
λ speed coefficient
ρ combustion gas density
ρ_p propellant density
ϵ ratio of corrosion
τ time increment

Subscript

0 parameters at 0 cross-section of grain
1 parameters at passage exit cross-section

t parameters at nozzle throat
s stagnation parameter

1

I. Preface

The purpose for predicting the performance of a solid propellant rocket motor is: to base on raw data such as structure of the motor, geometrical shape and dimensions of the grain, characteristics of propellant, etc. and calculate the changes with respect to time and their distribution along the length of the combustion chamber for parameters such as combustion gas pressure p, flow speed v, density ρ and temperature T during motor operating period.

Great advances have been achieved in the development of performance algorithms throughout the years. In earlier days the performance algorithms were built on the basis of quasi-steady flow and zero-dimension simplification [1]. Then, a one-dimensional model was adopted for conditions with larger volume filling coefficient and rather distinctive corrosion combustion phenomenon. A group of ordinary differential equations [2,5] could be obtained when conducting quasi-steady simplification on the basis of a one-dimensional model, and generally they could be solved using the Runge-Kutta or the Merson method [7]. If the unsteady effects are considered on the basis of the one-dimensional model, then the group of performance control equations are of first-order, linear hyperbolic partial differential equations, and the finite-difference and the characteristic-line method could be applied to solving them [8].

This article concentrates on the introduction of general algorithms for quasi-steady and unsteady equations, which is the Time-Space Alternate Algorithm. It was developed on the basis of the Triple-Loop Iteration Algorithm. Since the grain and performance calculations are closely related and indivisible, a general two-dimensional grain calculation procedure was employed in these calculations.

II. Triple-Loop Iteration and Time-Space Alternate Algorithms

1. Motor Model and Its One-Dimensional Performance Control Equations

Select motor model as depicted in Figure 1.

The following assumptions are made for the flow field inside the combustion chamber: combustion gas is ideal gas; flow is one-dimensional in the grain passage;flow process is frictionless, adiabatic, chemically nonreactive and homogeneous gaseous flow; the x-axis component of momentum of combustion gases generated on the combustion surface is zero. The performance control equations can be derived as:

$$\frac{\partial}{\partial t}(\rho A_p) + \frac{\partial}{\partial x}(\rho A_p v) = \rho_p r \frac{\partial A_b}{\partial x} \tag{1}$$

$$\frac{\partial}{\partial t}(\rho v A_p) + \frac{\partial}{\partial x}(\rho v^2 A_p + p A_p) = p \frac{\partial A_p}{\partial x} \tag{2}$$

$$\frac{\partial}{\partial t}\left[\rho A_p\left(\frac{v^2}{2}+E\right)\right] + \frac{\partial}{\partial x}\left[\rho v A_p\left(\frac{v^2}{2}+H\right)\right] = \rho_p r \frac{\partial A_b}{\partial x} H_p \tag{3}$$

$$p = \rho R T \tag{4}$$

If $v \ll a$, $\rho \ll \rho_p$, $\Delta A_p \ll A_p$ (within combustion gases resident time), the operation process of motor can be considered quasi-steady and the above equations can be simplified as:

$$\frac{d}{dx}(\rho A_p v) = \rho_p r \frac{dA_b}{dx} \tag{5}$$

$$\frac{d}{dx}(\rho v^2 A_p + p A_p) = p \frac{dA_p}{dx} \tag{6}$$

$$\frac{d}{dx}\left[\rho v A_p\left(\frac{v^2}{2}+H\right)\right] = \rho_p r \frac{dA_b}{dx} H_p \tag{7}$$

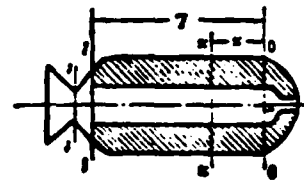$$p = \rho R T \tag{8}$$

Figure 1. Schematic of solid propellant rocket motor

2. Triple-Loop Iteration Algorithm

For adiabatic flow, the energy equation (7) in the one-dimensional quasi-steady performance control equations (5)-(8) can be simplified as:

$$c_p T + v^2/2 = c_p T_r \tag{9}$$

Then, only the continuity and momentum equations in the group are in differential form. Now let's select the mass flow rate $\dot{m}$ and p pressure as variables ,and change the continuity and momentum equations into the

3

following calculation forms:

$$\frac{d\dot{m}}{dx} = \rho_{r} r \frac{dA_{b}}{dx} \tag{10}$$

$$\frac{dp}{dx} = \frac{1}{A_{p}(a^{2}-v^{2})} \left\{ \rho v^{2} a^{2} \frac{dA_{p}}{dx} - \rho_{r} r \frac{dA_{b}}{dx} v \left(2a^{2}+(\gamma-1)v^{2}\right) \right\} \tag{11}$$

Every unknown parameter can be expressed as a function of $\dot{m}$ and p using the energy and state equations and other well known formulae.

The solving of performance equations is a boundary value problem rather than an initial value one; therefore the test-firing method is adopted. First, assume that the test value of head presure p_{0} can be estimated according to the following formula:

$$p_{0} = \left\{ \frac{\rho_{r}a_{1}A_{b}a_{0}}{A_{p}} \frac{2(\gamma+1)}{\gamma} \frac{1}{I(\lambda_{l})} \right\}^{\frac{1}{1-n}} \tag{12}$$

where

$$I(\lambda_{l}) = \int_{0}^{\lambda_{l}} \frac{4(1-\lambda^{2})}{(1+\lambda^{2})^{2-n}\left(1-\frac{\gamma-1}{\gamma+1}\lambda^{2}\right)^{n} \epsilon(\lambda)} d\lambda \tag{13}$$

and λ_{l} is determined by the following formula:

$$J = \frac{A_{l}}{A_{pl}} = \lambda_{l} \left(1-\frac{\gamma-1}{\gamma+1}\lambda_{l}^{2}\right)^{\frac{1}{\gamma-1}} \left(\frac{\gamma+1}{2}\right)^{\frac{1}{\gamma-1}} \tag{14}$$

The test value of p_{0} at time t_{1} can be obtained by selecting the p_{0} value that satisfies the flow conditions at time t_{0}. As to the p_{0} test values at time t_{2} and beyond, they can be obtained by using the p_{0} values at two previous time instants and applying the proportionality method, which is:

$$p_{0}(t_{m}) = p_{0}(t_{m-1}) \frac{p_{0}(t_{m-1})}{p_{0}(t_{m-2})}, \quad (m=2, 3, \cdots) \tag{15}$$

At any time instant, the mass flow rate across the O cross-section should be equal to the combustion gas generation rate at the motor head, then

$$\dot{m}_{0} = A_{b0}\rho_{r}a_{1}p_{0}^{n} \tag{16}$$

Once the grain head boundary conditions p_{0} and $\dot{m}_{0}$ are determined, equations (10) and (11) can be solved as initial value problems using the Merson method. Then adjust p_{0} value according to the boundary conditions at the grain tail. In order to do this, the combustion gas

4

generation rate $\dot{m}_b$ and exhaust rate $\dot{m}_e$ must be obtained,

$$\dot{m}_b = \dot{m}_i + \dot{m}_d$$
$$\dot{m}_e = C_b p_{sl} A_t$$

where $\dot{m}_d$ is the combustion gas generation rate at the cross-section of grain tail. Since the flow from the cross-section of grain exit to nozzle throat is also considered quasi-steady, $\dot{m}_e$ should be equal to $\dot{m}_b$. If the calculated values for $\dot{m}_e$ and $\dot{m}_b$ are not equal, then this shows that the assumed value for p_0 is not reasonable and should be adjusted. The proportionality method can be used for the first adjustment of the p_0 test value, that is:

$$p_0^{(2)} = p_0^{(1)} \dot{m}_b / \dot{m}_e \tag{17}$$

After the number of iterations exceeds two, interpolation formula can be used to adjust p_0 value. At this time, let $\Delta \dot{m} = \dot{m}_e - \dot{m}_b$, then

$$p_0^{(n)} = p_0^{(n-1)} + \Delta m^{(n-1)} \frac{p_0^{(n-1)} - p_0^{(n-2)}}{\Delta m^{(n-2)} - \Delta m^{(n-1)}} \tag{18}$$

$$(n = 3, 4, \cdots)$$

The iteration continues until $\Delta \dot{m}$ is less than a designated value.

When the solution at time t_{m-1} has been obtained and the solution at time t_m is continued, the geometrical parameters at time t_m should be obtained by grain calculations first. The grain thickness burned at each node during time Δt can be obtained according to the following calculation:

$$\Delta y_i = r_i \Delta t$$

where r_i is the average speed of combustion during time Δt and it is dependent upon the speed of combustion at time t_m. However, the speed of combustion at time t_m is affected by combustion gas parameters and thus by Δy_i, it must be calculated by the iteration method. We employed the scheme of simple prediction and multiple adjustments. The specific formulae are:

$$r_i^{(0)}(t_m) = r_i(t_{m-1}), \quad (m = 1, 2, \cdots)$$
$$r_i^{(n)}(t_m) = \frac{1}{2}(r_i(t_{m-1}) + r_i^{(n-1)}(t_m)), \quad (n = 1, 2, \cdots)$$

In applying the Merson method to conduct numerical integration, the grain geometrical parameters and their derivatives with respect to x at certain points between two nodes must be used. These data are obtained from the LaGrange quadratic polynomial interpolation and

5

their corresponding numerical differential equations.

3. Time-Space Alternate Algorithm

The one-dimensional, unsteady performance control equations (1)-(4) are of first-degree, near-linear, hyperbolic partial differential equations. If the characteristic-line method is used for solution, the time increment must be set very small due to the limitation of stability conditions of the difference scheme. Ten thousand or more calculation steps are required for a typical motor. This is very inconvenient and sometimes even unacceptable.

The essence of the Time-Space Alternate Algorithm is to reduce partial differential equation to ordinary differential equation. High accuracy for time and space increments can be obtained. In reference [6],Burstein used a similar method to solve hyperbolic equations and obtained third-degree accuracy for both time and space increments. This article applied the Time-Space Alternate Algorithm and obtained not only fourth-degree accuracy for time and space increments, but also nicely combined the solving methods of unsteady and quasi-steady equations.

In the Time-Space Alternate Algorithm, ρ, v and p were selected as calculation variables. First of all,equations (1)-(3) were changed to:

$$\frac{\partial \rho}{\partial t} + v \cdot \frac{\partial \rho}{\partial x} + \rho \frac{\partial v}{\partial x} = \alpha \qquad (19)$$

$$\frac{\partial v}{\partial t} + v \frac{\partial v}{\partial x} + \frac{1}{\rho} \cdot \frac{\partial p}{\partial x} = \beta \qquad (20)$$

$$\frac{\partial p}{\partial t} + \gamma p \frac{\partial v}{\partial x} + v \frac{\partial p}{\partial x} = \psi \qquad (21)$$

where $\quad \alpha = \frac{1}{A_p}(\rho_p - \rho)qr - \frac{1}{A_p}\rho v\frac{\partial A_p}{\partial x}$

$\beta = -\frac{\rho_p v qr}{A_p \rho}$

$\psi = \frac{qr}{A_p}\left(\rho_p \gamma RT_b + \frac{\gamma-1}{2}\rho_p v^2 - p\right) - \frac{\gamma p v}{A_p}\frac{\partial A_p}{\partial x}$

Then equations (19)-(21) were written in calculation forms, thus

$$\frac{\partial \rho}{\partial x} = \frac{1}{a^2-v^2}\left[-\frac{a^2-v^2}{v}\frac{\partial \rho}{\partial t} - \rho\frac{\partial v}{\partial t} + \frac{1}{v}\frac{\partial p}{\partial t}\right]$$
$$+ \frac{1}{a^2-v^2}\left[\frac{1}{v}(a^2-v^2)\varepsilon + \rho\beta - \frac{1}{v}\psi\right] \qquad (22)$$

6

$$\frac{\partial v}{\partial x} = \frac{1}{a^2-v^2}\left[v\frac{\partial v}{\partial t} - \frac{1}{\rho}\frac{\partial p}{\partial t}\right] + \frac{1}{a^2-v^2}\left[-v\beta + \frac{1}{\rho}\psi\right] \qquad (23)$$

$$\frac{\partial p}{\partial x} = \frac{1}{a^2-v^2}\left[-\gamma p\frac{\partial v}{\partial t} + v\frac{\partial p}{\partial t}\right] + \frac{1}{a^2-v^2}(\gamma p\beta - v\psi) \qquad (24)$$

at any prescribed time instant, if the values of $\partial p/\partial t$, $\partial v/\partial t$ and $\partial p/\partial t$ in equations (22)-(24) have already been obtained. Thus, the equations can be considered ordinary differential equations with respect to x. With this in mind, the solutions can be obtained by the aforementioned Triple-Loop Iteration Algorithm. After obtaining the values of ρ, v, and p in the axial direction at each node and, respectively, substracting from them the values of ρ, v and p at the same node but at a previous time instant, and then divided by the time increment between the two time instants, the average rate of change of ρ, v and p at any node between two time instants can be obtained. Using these average rates of change as the approximate values for $\partial p/\partial t$, $\partial v/\partial t$, and $\partial p/\partial t$ and substituting them into equations (22)-(24) for solution based on the above algorithm. Thus, repetitive and alternating calculations can be conducted according to time and space increments so as to adjust the values of $\partial p/\partial t$, $\partial v/\partial t$, and $\partial p/\partial t$ iteratively. Once a certain accuracy is satisfied, the calculations for the next time instant begin and proceed till the motor stops.

If equations (22)-(24) are expressed in vector forms, then

$$\frac{\partial \vec{u}}{\partial x} = A\frac{\partial \vec{u}}{\partial t} \qquad (25)$$

When discussing the stability of the difference scheme, the above equation is usually simplified as:

$$\frac{\partial \vec{u}}{\partial x} = A_0 \frac{\partial \vec{u}}{\partial t} \qquad (26)$$

where A_0 is a constant matrix.

When using the Time-Space Alternate Algorithm to solve model equation (26), it is equivalent to applying the difference scheme:

$$\frac{\vec{u}_{j+1}^{n+1}-\vec{u}_{j}^{n+1}}{h} = \frac{A_0}{6}\left[\frac{\vec{u}_{j}^{n+1}-\vec{u}_{j}^{n}}{\tau} + 4\frac{\vec{u}_{j+1/2}^{n+1}-\vec{u}_{j+1/2}^{n}}{\tau} + \frac{\vec{u}_{j+1}^{n+1}-\vec{u}_{j+1}^{n}}{\tau}\right] \qquad (27)$$

7

Here the difference scheme is unconditionally stable with respect to the model equation. Through actual calculations, it is proven that for actual equations, the above discussions also apply.

The Triple-Loop Iteration Algorithm was adopted in consideration of the solving of equations with respect to x in the Time-Space Alternate Algorithm. Therefore, only the portion different from the algorithm for quasi-steady equations is introduced here.

The necessary initial conditions for the Time-Space Alternate Algorithm include the values of ρ, v and p at each node at the initial time instant and the values of $\partial\rho/\partial t$, $\partial p/\partial t$ and $\partial v/\partial t$. When conducting calculations immediately following the startup of the motor, the above initial conditions could be determined by the calculations for the startup process. However, when the calculations were started directly at the steady state of the motor, we assumed that the flow field inside the combustion chamber reached steady state at the initial instant; thus the values of $\partial\rho/\partial t$, $\partial v/\partial t$ and $\partial p/\partial t$ at each node can be assigned zero and the values for ρ, v and p at each node obtained by the Triple-Loop Iteration Algorithm were used as the initial values.

The determination of the value p_0 in the grain head boundary conditions is the same as that of the Triple-Loop Iteration Algorithm. But the value of ρ_0 and v_0 is determined by using the following formula:

$$\rho_0 = p_0/RT_0$$
$$v_0 = \frac{A_{bo}\rho_{P}a_1 \rho_0^2}{\rho_0 A_{P_0}}$$

At time t_m, the test values for $\partial\rho/\partial t$, $\partial v/\partial t$ and $\partial p/\partial t$ values at each node are substituted by the average values $\Delta\rho/\Delta t$, $\Delta v/\Delta t$ and $\Delta p/\Delta t$ between time t_{m-1} and t_{m-1}. After the values of ρ, v and p at each node at time t_m were obtained they are then adjusted. The adjustment formulae are:

$$\left(\frac{\partial\tilde{a}}{\partial t}\right)_i^{(1+s)} = \frac{\tilde{a}_i^m(t_m) - \tilde{a}_i(t_{m-1})}{t_m - t_{m-1}}$$

$$(m = 1, 2, \cdots; \ s = 1, 2, \cdots)$$

Adjustment can be conducted repetitively until the difference of ρ, v and p values between two consecutive iterations is smaller than a prescribed value.

8

III. Grain Calculation

The purpose for grain calculation is to obtain the grain geometrical parameters required for the motor performance calculation. For different types of motor performance calculation, not only the required grain geometrical parameters are different, the type of coordination between the grain and motor performance calculation is also different. For zero-dimensional performance algorithm, the required grain geometrical parameters generally correspond to the value of grain combustion surface of a given burned grain thickness. Then, the grain and performance calculations can be conducted separately. However, for the performance algorithm of one-dimensional and variable cross-sectional passage the required grain geometrical parameters generally correspond to the values of the combustion circumference of the local burned grain thickness and passage surface area. With corrosion combustion present, the grain and performance calculations are already closely related and indivisible, and they must be conducted alternately through iteration.

The performance algorithm introduced in this article incorporates the grain calculations. For this reason the authors proposed a two-dimensional general algorithm for grain calculation [9]. To expand from the basis of this algorithm, three-dimensional calculation problems such as the double-arc transient head seal and the tail-end surface, which is located at the ellipsoid behind the motor and does not restrict combustion.

IV. Examples and Discussions

Test runs of this computer program on three different real motors were conducted. Both Triple-Loop Iteration and Time-Space Alternate Algorithms were applied on each motor. For example 1 and 3, since their performance parameters during the operation period changed little with respect to time and the results obtained from both algorithms differed little, only the results obtained from the Triple-Loop Iteration Algorithm are presented. As for Example 2, the results obtained from both algorithms are presented.

Example 1.   The grain is star-shaped, two-dimensional and internal cavity-filled. The head portion is double-arc transient head seal. The tail-end surface is located at the ellipsoid behind the motor and allows unrestricted combustion. See Figure 2 for the results of calculation.

Example 2.   The grain is wheel-shaped and internal cavity-filled. Both the head and tail-end surfaces are located at the cylindrical section of the motor and both allow unrestricted combustion. See Figure 3 for the results of calculation.

Example 3.   The grain is of inner/outer surfaces simultaneous combustion and single tubular fill. Both the head and tail-end surfaces restrict combustion. See Figure 4 for results of calculation.
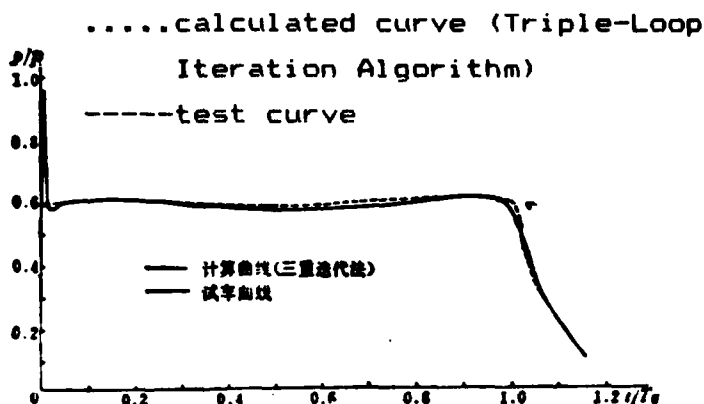

Figure 2. Pressure vs time diagram of solid
rocket motor for Example 1.

It can be observed from the calculated results that when changes with respect to time in the performance parameters are more significant (Example 2), there are marked differences between results obtained from the quasi-steady ordinary differential equations (Triple-Loop Iteration Algorithm) and those from the unsteady ordinary differential equations (Time-Space Alternate Algorithm), and the latter had a calculation accuracy about 1.6% higher than that of the former.
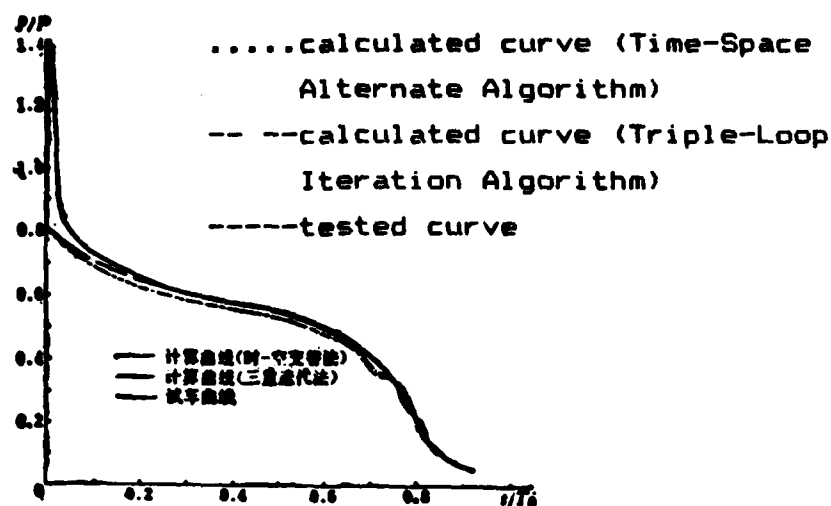
..... calculated curve (Time-Space Alternate Algorithm)

-- -- calculated curve (Triple-Loop Iteration Algorithm)

----- tested curve

Figure 3. Pressure vs time diagram of solid rocket motor for Example 2.

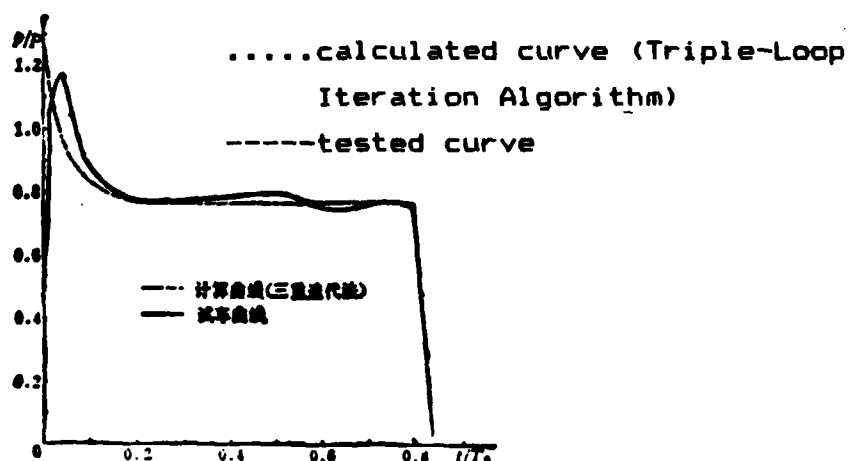..... calculated curve (Triple-Loop Iteration Algorithm)

----- tested curve

Figure 4. Pressure vs time diagram of solid rocket motor for Example 3.

References

[1] Barrero, M., Jaumotte, A., Fraeijs de Veubeke, B. and J. Vandenkerckhove, Rocket Propulsion, Elsevier Publishing Company, (1960).

[2] A. A. 寺介和夫著, 冥崎藤译, 固体大量炽变速氧气体动力学, 国防工业出版社, (1979).

[3] A. M. 楼尼亚诺夫著, 余金顺等译, 固体大量变速氯, 国防工业出版社, (1981).

[4] Rayzberg, B. A., Yerokhin, B. T., Samsorov, K. P., Principles of the Theory of Procedures in Rocket Systems on Solid Fuel, AD 766567, (1973).

[5] Coats, D. E. et al, A Computer Program for the Prediction of Solid Propellant Rocket Motor Performance, Vol. I, ADA015140, (1975).

[6] Burstein, S. Z. and Mirin, A. A., Third Order Difference Methods for Hyperbolic Equations, J. Comput. Phys. Vol. 5, No. 3, (1970).

[7] 王柏, 鱼中枝, 三重道代内算道计算方法及程序, 推进技术, 4期 (1983).

[8] Peretz, A., Kuo, K. K., Caveny, L. H., Summerfield, M., Starting Transient of Solid Propellant Rocket Motors with High Internal Gas Velocities, AIAA J. Vol. 11, No. 12, (1973).

[9] 王柏, 鱼中枝, 二维流场适用计算方法及程序, 推进技术, 3期 (1982).

STUDY ON ALGORITHMS FOR PREDICTION OF SOLID PROPELLANT ROCKET MOTOR PERFORMANCE

Wang Xin and Zhang Zhongqin

(Beijing Institute of Aeronautics and Astronautics)

Abstract

Two algorithms for prediction of solid propellant rocket motor performance are introduced. Triple Loop Iteration Algorithm is applied to solution of quasi-steady equations$(5)\sim(8)$. Its computer program comprises a procedure with three iterative loops. Time-Space Alternate Algorithm can be applied to soluting both quasi-steady equations and unsteady equations $(22)\sim(24)$. If $\partial\rho/\partial t, \partial v/\partial t, \partial p/\partial t$ in equations $(22)\sim(24)$ are given, equations $(22)\sim(24)$ will be reduced to ordinary differential equations. They can be solved by Merson's method. When $\Delta\rho/\Delta t, \Delta v/\Delta t, \Delta p/\Delta t$ are approximated to $\partial\rho/\partial t, \partial v/\partial t, \partial p/\partial t$, this algorithm for model equation

$$\frac{\partial\vec{u}}{\partial x} = A_0 \frac{\partial\vec{u}}{\partial \tau}$$

corresponds to the finite difference scheme

$$\frac{\vec{u}_{j+1}^{n+1}-\vec{u}_j^{n+1}}{h} = \frac{A_0}{6}\left[\frac{\vec{u}_j^{n+1}-\vec{u}_j^n}{\tau} + 4\frac{\vec{u}_{j+1/2}^{n+1}-\vec{u}_{j+1/2}^n}{\tau} + \frac{\vec{u}_{j+1}^{n+1}-\vec{u}_{j+1}^n}{\tau}\right]$$

It is an unconditionally stable scheme.

A general two-dimensional grain calculation method is introduced for calculation of grain. A comprehensive computer program for above mentioned methods has been written and applied to calculating the performance of three different motors. The results of the numerical examples are consistent with the experimental data.

END

DTIC

6 - 86